TiPS

Nano Composite Fe-Co-V/Zeolite as a Nano Carrier for Folic Acid Drug Controlled Release

Shima Zangeneh Yousef Abadi[1], Mohammad Kazem Mohammadi[1*], Haman Tavakkoli[1]

[1]Department of Chemistry, Ahvaz Branch, Islamic Azad University, Ahvaz, Iran.

Abstract

Having large reserves of zeolites is one of the comparative advantages of Iran which provides economic justification for its use in a variety of applications, including medical and pharmaceutical fields such as artificial kidney manufacturing, wound dressing, controlled drug release, and bone tissue engineering. In this study, in order to protect folic acid drug (folate) in digestive system acidic environments, zeolite nano carrier (Fe-Co-V/zeolite) was used. After being dissolved in ethanol, a certain amount of this drug was placed on zeolite and extracted at different time periods. The release rate of folic acid in similar conditions of stomach and intestine was measured by placing samples of zeolite containing this compound in aqueous solution with the acidic pH of 5.4 and 8.9. The release rate in acidic medium was 17% higher than the release of drug in alkaline medium. SEM test was performed to measure the morphology of the pores and to measure the changes in the acidic grade and evaluate the buffering properties of this material. The findings revealed that folic acid was very unstable in acidic conditions and the use of zeolite significantly protected folic acid. This can be to note that the highly porous structure of zeolite can affect the initial absorption attributed to the nature of automatic control of the acidic degree in the tolerable range of the drug (chemical protection). The release of desired amount of vitamins in an area of chemical protection is also important.

1. Introduction

In recent years, the use of nanoparticles produced from mineral or organic materials in drug delivery, peptides-proteins, genes and vaccines has attracted much attention (1-5). In general, the nanoparticles used in drug delivery have a size less than 1,000 nanometers and with the help of chemical reaction activators, are able to be trapped inside, dissolved, wrapped, or adsorbed on their surface.

According to the internal structure of nanoparticles, they can be classified into two

groups: matrix and vesicular. Matrix nanoparticles are homogeneous systems in which chemical reaction activators are dissolved or dispersed throughout the particles. Vesicular nanoparticles, also called nano capsules, are heterogeneous systems that are surrounded by mineral or organic membranes with the help of active materials in an aqueous or oily cavity (6-7).

Dimensions and surface chemistry play an important role in determining the function of drug-containing nanoparticles and their therapeutic efficacy. Nanoparticles with intravenous application, due to their sub-micro dimensions, have very permeability and aggregation. This means that they tend to accumulate in target areas such as tumor

Corresponding Author: Mohammad Kazem Mohammadi, Department of Chemistry, Ahvaz Branch, Islamic Azad University, Ahvaz, Iran.
Email: mkmohamadi@gmail.com

tissue and damaged organs with the help of biological mechanisms and show their proper effectiveness (8).

Nanoparticles with a very small size (less than a hundred nanometers) prevent the drug from being absorbed by the reticuloendothelial system (part of the body's immune system: composed of a group of cells such as phagocytosis) that excrete excess substances and as a result, can increase blood circulation (9). When consumed orally or locally (for example, by inhalation, cornea, *etc.*), due to the large specific surface area, they usually have a longer durability and provide high concentrations of local drugs that increase the availability of drug amount in the desired location (10).

Nanoparticle dimensions also have an important role in the drug delivery at the cellular level. Entrance of nanoparticles into cells (cancer cells, intestinal cells and others) depends on its size. The smaller the particle, the more increase in the rate of entry into the cell (11-12). As a result, nanoparticles containing of active materials may have more cell toxicity (due to higher cell absorption) than tumor cells (13).

In other words, nanoparticles - based on their small size - have the ability to cross physiological barriers (e.g., gastrointestinal, blood-brain and other barriers) and this increases the availability of the drug at the desired location (14).

Zeolites are hydrous porous alumino silicate that contain alkaline or alkaline earth metal elements, especially sodium, potassium, magnesium, calcium, strontium and barium. (15) Most zeolites with low or medium Si (Si to Al ratio of 1.5/1 and 2/1.5, respectively) decompose in acidic solutions with pH below 3 (16-17).

Some compounds with large amounts of Si, such as clinoptilolite and mordenite, are stable at pH range of 2 and are stable for shorter periods, even at pH below 2. This material is neutralized by the placement of monovalent or divalent cations such as K^+, Ca^{2+}, Mg^{2+} and Na^+ (18).

Exchangeable cations are not stable within the zeolite lattice and exchange in the vicinity of other high concentration cations (19-20). The biocompatibility of some zeolites and the manufacture of artificial kidneys and bone tissue by them in recent years shows the potential of this material for use in medical and surgical applications. Other medical applications of this substance include the development of anti-cancer, anti-diarrheal, and anti-diabetic drugs as well as their use as biosensors and wound dressings.

It must be noted that the use of zeolite for manufacturing the drug delivery systems is one of the largest and newest medical uses of this material. The method of absorption and release of drugs such as metronidazole, sulfamethoxazole and ibuprofen in various zeolites has been studied in recent years (21-24).

In terms of solubility, vitamins are divided into two groups: fat-soluble vitamins and water-soluble vitamins. Most vitamins are absorbed in the end part of the gastrointestinal system and most of them (especially folate) are sensitive to pH changes in this device. Therefore, a carrier which can pass this vitamin from the beginning of the gastrointestinal system, ensures the stability of this vitamin for longer periods.

The anti-acid property of clinoptilolite as one of the zeolites has been proven in the release of drugs such as aspirin, metronidazole and sulfamethoxazole in the recent ten years (25-27). In continuation of our work on the medicinal chemistry (28-31), we synthesized zeolite nano structure as a carrier for folic acid and evaluated its stability and its release in an environment similar to the stomach and intestines medium.

2. Materail and methods
2.1. Instruments

Fourier transform infrared (FT-IR) patterns were obtained on a Perkin Elmer BX-II spectrophotometer (Perkin Elmer Company, USA 400-4000 Cm-1). A FESEM, Zeiss SIGMA VP-500 (sigma company, USA) equipped with side detectors of EDS and high-resolution elemental mapping was utilized to characterize surface morphology and elemental compositions. UV-Vis DRS was performed by a UV-Vis spectrophotometer (Avaspec-2048-TEC. 200-1100 nm. Avantes company, Holland). The morphological features of sample were investigated with a Zeiss (EM10C -Germany) transmission electron microscope (TEM) operating at 100 kV.

2.2 Experimental

The zeolite sample was initially prepared as blocks from different parts of the Semnan mine. The rocks were crushed by mechanical methods and powders to particle size of 700 to 850 microns using electric mortars and ball mills. Then all the particles were dried in the oven for 2 hours at 105 °C. Then 0.1 g of vanadium pentoxide (V2O5) was dissolved in one liter of 3 M sodium hydroxide solution.

The resulting pale yellow solution was filtered to remove solid impurities. At this stage, the solution was titrated with 6 M nitric acid to PH=6. At this time, most of the vanadium is in the form of a decavanadite solution complex (pink color) (V10O286). The zeolite powder was then added to a balloon containing decavanadite solution and equipped with a magnetic stirrer and the contents of the balloon were stirred for 24 hours at 60 °C.

At this time, almost all decavanadite ions are adsorbed on the zeolite. All zeolites became uniformly pink. At this time, a molar solution of iron nitrate and cobalt nitrate was added drop wise to the contents of the stirring flask. The contents of the balloon were stirred for another 5 hours at 60 °C. Finally, the contents of the balloon were filtered and air-dried and placed in a reactor and regenerated with hydrogen at 20 bar and 500 °C for 5 hours. After the reduction step, structure and morphology of the catalyst were studied by XRD and TEM devices.

3. Results and Discussion

3.1. Nano Zeolite Characteristic

The types of chemical bonds and vibrational properties of the synthesized samples were investigated using FT-IR spectroscopy. Figure 1. shows the FT-IR spectra of Fe-Co-V / Zeolite CNS at wavelengths of 400-4000 Cm^{-1}.

This peak also depicts the internal quadrilateral flexural vibration of the TO4 zeolite structure. It also shows the presence of Al^{+3} and SiO4 in the zeolite. Peaks at 665 Cm^{-1} can refer to Si-O-Si, while peaks at 715 and 728 Cm^{-1} can be symmetrical due to traction (T-O-T, T=Si, Al). The peaks of 835 and 837 Cm^{-1} can be attributed to the bending vibrations of Fe-OH.

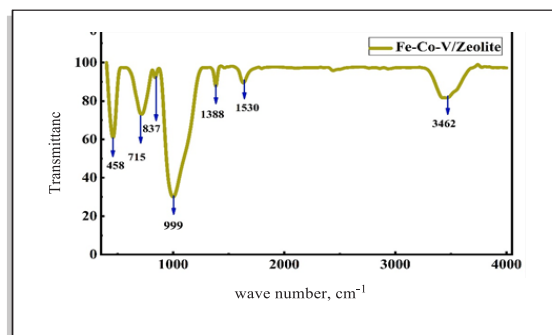The peaks of the solid bands seen around

Figure 1. IR spectrum of Fe-Co-V / Zeolite nano structure.

995 and 999 cm^{-1} can be attributed to the overlap of the symmetrical vibrations of the Si-O (bridging) and Si-O- (non-bridging) joints. The peaks of 1383 and Cm^{-1} 1388 can be attributed to the bending vibrations of C-N. For Fe-Co-V / Zeolite, a weakly observed peak may be due to the weaker interaction of V metal with the zeolite surface. The peaks at 1530 and 1622 cm^{-1} can be related to the stretching vibrations of water molecules, while those at 3416 and 3462 Cm^{-1} are due to OH stretching vibrations.

The peak appeared in 2355 cm^{-1} may be due to the interaction between Fe-Co-V and TO4 ions in zeolite. Due to the weak covalent bond in metal V, this peak was observed in this very weak spectrum.

The morphological characteristics of the as-synthesized samples were studied by FESEM. Figure 2. displays FESEM images of Fe-Co-V/ Zeolite in two different magnifications. Figure 2a presents the overall image of Fe-Co-V/Zeolite consisting of an aggregation of irregular shapes. The high-resolution image is shown in Figure 2b indicates rough surfaces for Fe-Co-V/Zeolite due to the formation of spherical nanoparticles with a size ranging from 20 to 60 nm.

The surface elemental distribution of as-synthesized samples was examined by FESEM-EDS mapping. Figure 3. shows FESEM images and the corresponding elemental mappings for Fe-Co-V/Zeolite CNS. Exhibits the uniform existence of Al, Si, Fe, Co, O, and V elements in the boxed surface area for Fe-Co-V/Zeolite sample. The quantitative elemental analysis for Fe-Co-V/ Zeolite was also carried out using recording EDX spectra as shown in Figure 3. Resulted spectra
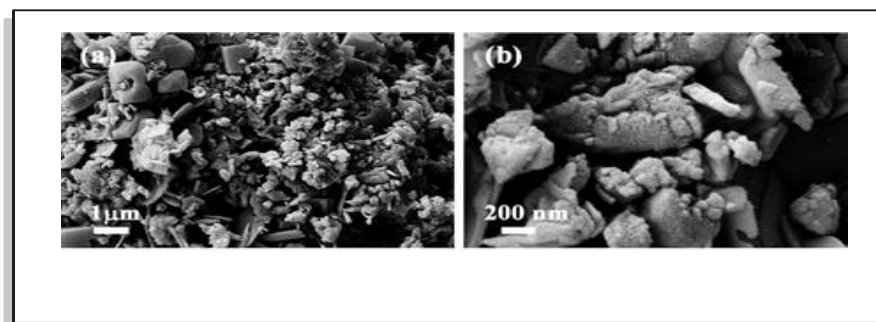
Figure 2. FESEM images of Fe-Co-V/Zeolite nano structure.

indicate the presence of Al, Si, Fe, Co, O, V in Fe-Co-V/Zeolite CNs, respectively. Table 1. summarizes the numerical analysis of EDX spectra for as-synthesized samples.

For the closer look of synthesized microstructures, used of transmission electron microscope (TEM). Transmission electron microscope image of Fe-Co-V/Zeolite, showed in the Figure 4. In the figure (a), TEM image of Fe-Co-V/Zeolite CNs to be observed with the 50 nm magnification. According to this figure, it can be said that the particles have an almost spherical surface morphology with the different particle sizes. TEM image of Fe-Co-V/Zeolite nano particles (figure b), to be observed with the 100 nm magnification. This image clearly shows that nano particles have an irregular surface morphology (Figure 4).

Nano graphene oxide (GO) have emerged as an important class of nano materials for a wide variety of industrial and medical applications. The use of GO (32) and functionalized GO with other compounds like metal groups, polymers (33), etc., in drug delivery and cellular imaging (34) has been reported. The drug delivery efficacy of Pt was enhanced through the introduction of poly ethylated GO (PGO), and the final weight ratio of DOX: Pt: PGO was optimized to 0.376:0.376:1. Drug release results indicated that both Pt and DOX release kinetics from pGO-Pt/DOX nanoparticles

were pH-dependent like the Fe-Co-V / Zeolite. In other cases, folic acid (FA) was linked to PEG (4,7,10-trioxa-1,13-tridecanediamine) to form FA–PEG, followed by coupling to the GO surface. Camptothecin (CPT) was further adsorbed on GO for use as a drug model in the delivery study. GO–FA indicated a high CPT loading capacity (37.8%). In vitro studies confirmed prolonged drug release over 200 h. Acidic pH (5.0) slowed the release of CPT from the nano carrier compared to that at physiological pH (7.4) (35).

3.2. Determining the Optimal Loading Amount

Initially, 0.1 g of zeolite nanostructure was placed in the vicinity of different concentrations of folic acid in the ratio of 1:3, 1:2, 1:1 prepared from the synthesis of the synthesized derivative in deionized water and evaluated its loading on nano structure at two different times (24 hr and 48 hr). For this purpose, a magnet was located into each balloon and each of the concentrations prepared from the compound along with the zeolite nano carrier was added to the reaction vessel.

Each balloon was closed and covered with aluminum foil, and then was placed on a stirrer at 200 rpm for 48 hours. After 48 hours, the samples were centrifuged at 10,000 rpm for 5 minutes. The top layer of each balloon was kept in a separate container according to the concentration added to
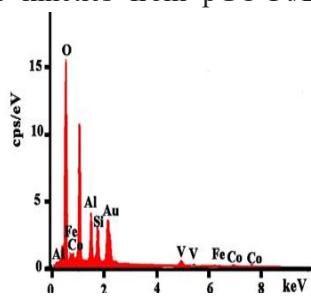
Table 1. EDX spectra table of Fe-Co-V/Zeolite nano structure.

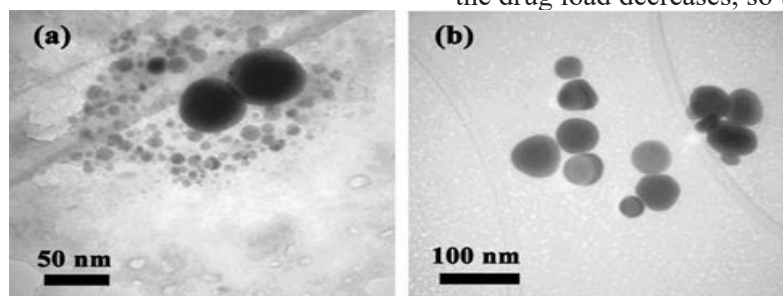| Sample	Al		Si		Fe	
	Wt%	σ	Wt%	σ	Wt%	σ
Fe-Co-V/Zeolite	12.3	0.2	10.1	0.2	5.2	0.8
Sample	Co		O		V	
	Wt%	σ	Wt%	σ	Wt%	Σ
Fe-Co-V/Zeolite	6.4	0.6	52.7	0.7	13.2	0.5
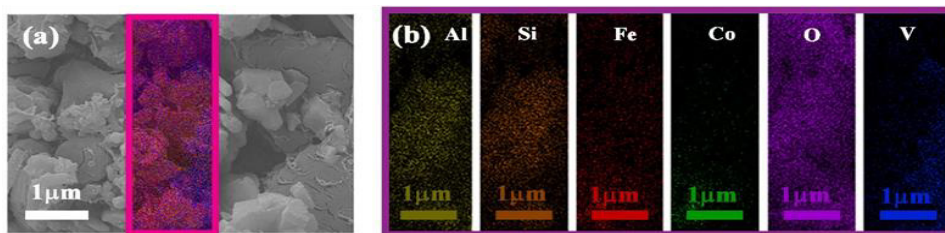
Figure 3. Elemental mappings for Fe-Co-V/Zeolite nano structure.

each balloon and kept in the refrigerator to analyze the load amount.

Thus, after the end of the loading time, the entire filtered top phase was diluted to 25 ml and with the spectrophotometer and its absorbance was obtained at a 350 nm. Finally, the nanostructures loaded in a vacuum oven were dried at 60 °C for 6 hours.

To draw the calibration curve, the drug loading percentage in the zeolite nanostructure was calculated from Equation 1. The nanostructures loaded in the vacuum oven were dried at 60 °C for 6 hr. The results show that the best drug load on the nanostructure in 24 hours in a ratio of 1:1 is 85%, because with increasing the delivery percentage, the drug load decreases, so this ratio is selected to

Figure 4. TEM image of Fe-Co-V/Zeolite.

analyze the drug release for the nanostructure. The results of loading tests are listed in Table 2.

FT-IR and EDX analyses were used to prove the drug load on the zeolite nano carrier (Figure 5, 6). As can be seen in Figure 5, the presence of the oxygen element in this analysis confirms the loading of the compound on the nanostructure as a nano carrier.

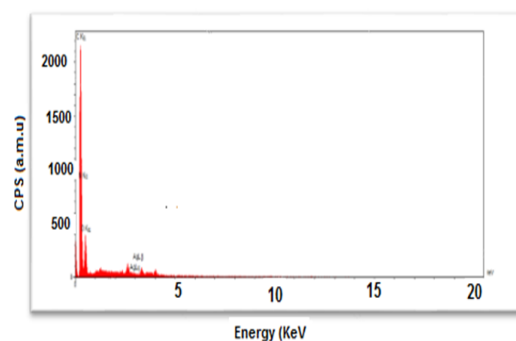### 3.3. Folic acid stability test

To 1 g of nano carrier of vanadium, iron, cobalt on zeolite substrate, 1 ml of solution with a concentration of 10 μg /l was added. The sample tube was placed at room temperature to evapo-

rate its solvent (ethanol). To measure the amount of folic acid carried by the nano carrier, folic acid was extracted with a suitable solvent. During extraction, the contents of each tube are poured into a new tube and the extraction is performed in a new tube. The method used to prepare the control sample for folic acid stability test was similar to the original sample preparation method. The only difference between the two methods is that the control sample was without zeolite.

Table 2. Drug delivery optimization in 24 hr and 48 hr.

no	Drug/nano carrier	Loading percentage in 24 hr	Loading percentage in 48 hr
1	1:1	85	81
2	1:2	78	72
3	1:3	53	49

Figure 5. EDX analysis of loaded nano Fe- Co-V/ zeolite.
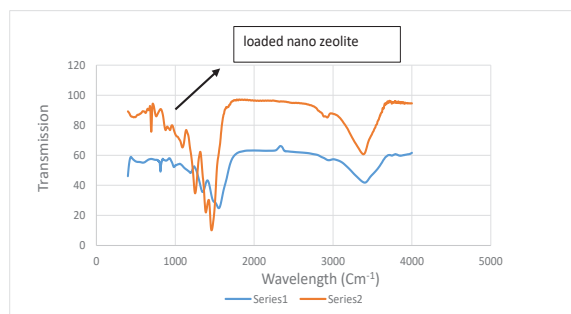
Figure 6. FT-IR spectrum of nano zeolite (blue curve) and loaded nano zeolite (orang curve).

3.4. Determination of compound release from nanostructures loaded in simulated fluids

Before examining the release of the compound in the simulated fluids, the calibration curve of this compound was obtained in each of the simulated fluids. Then, using the method presented in the previous section, the drug release percentage was obtained using the standard amount of absorption, drug concentration and, as a result, the amount of drug released in the phosphate solution. The measurement of the released compound continued until the concentration of the solution changed.

In order to calculate the percentage of drug release at the specified times, after each load, the absorbed drug was obtained using a spectrophotometer (Figure 7) and then the concentration of drug released in the buffer medium at each step by the values calculated from the equation of the drug absorption calibration curve (Figure 8). Using the initial composition rate, the release percentage of the compound was obtained using the following equation.

Equation 1:

$$\text{drug delivery}(\%) = \frac{\text{released drug}}{\text{loaded drug}} \times 100 \qquad \text{Eq.1}$$
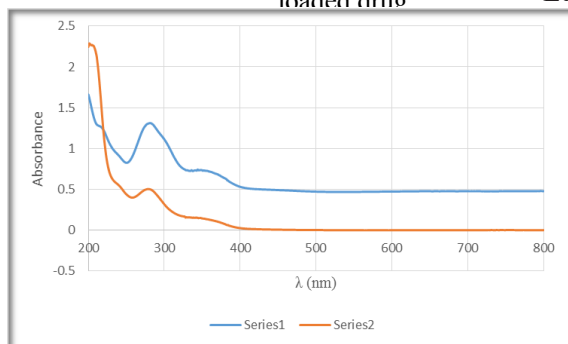
Figure 7. UV-Vis spectrum for loaded drug differences before (blue curve) and after (orange curve) loading

Table 3. UV absorption of different concentrations at buffer medium.

Abs.	Conc.(mg/ml)
0.0298	1.5625
0.11	3.125
0.14	6.25
0.56	12.5
1.32	25
1.52	50

To make an aqueous solution with a pH of 1.7, 1 N hydrochloric acid with a purity of 37% was used. Firstly, in order to investigate the effect of zeolite on the medium pH changes, 5 g of it was placed in 100 ml of the mentioned acidic solution and its pH was measured and recorded in a 30-minute sequence from the time of addition. To evaluate the release of folic acid in an acidic medium, initially 5 ml of 10 g/ml solution was added to 5 g of nano carrier.

The vessel was placed under the hood for evaporate the ethanol. The obtained sample was added to 100 ml of the mentioned acidic solution under a stirring at a rate of 50 rpm. Every 30 minutes, Sampling was performed to measure the folic acid released into the solution (until 330 minutes). All samples were stored in a refrigerator at 3 °C and injected to HPLC, respectively. The amount of vitamin present in the environment was calculated from the curve under Area obtained by HPLC.

3.5. Folic acid evaluation and measurement

The approximate chemical composition of the samples used in this experiment was measured by EDX method. Scanning electron microscopy (Holland, Philips, XL30, SEM) was used to study
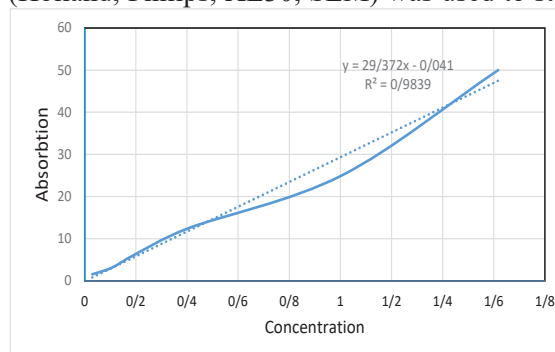
Figure 8. Standard curve of loaded drug in buffer medium.
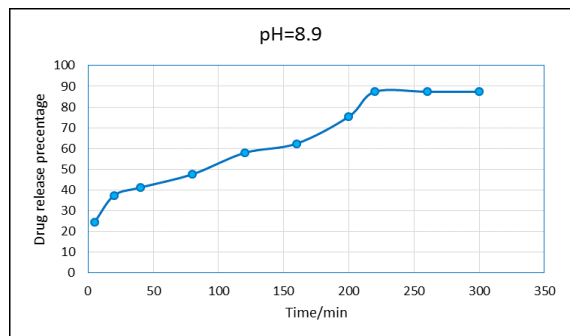
Figurer 9. Diagram of drug release from nano carrier in basic medium at pH=8.

the porosity and microstructure of the particles. The amount of vitamin in stability and release tests was measured by 1200 Agilent series (HPLC) method. So that, after the system setup for folic acid detection, system parameters include constant and mobile phase, mobile phase ingredient ratio, peak recording time and etc. Proved in appropriate quantities.

The electron microscopic image of the zeolite powder particles is shown in Figure 2. Porosities smaller than 5 micrometers can be seen in this image. Studies with more magnifications showed that the smallest porosities in the measurable range are about 1 micrometer. These porosities can be considered as suitable places for absorbing and transporting vitamins. Approximate chemical analysis performed by EDAX method shows the ratio of average amounts of silicon to aluminum equal to 5/2.

3.6. Drug release in basic pH

Figure 9 shows the amount of release (folic acid) in the basic medium. As can be seen in this figure, the release rate of the vitamin in the zeolite sample is initially very high and increases over time. In the sample containing zeolite, the

Table 4. UV absorbent amount of different concentrations in acidic medium.

| Abs.	Conc.(mg/ml)
0.11	1.5625
0.23	3.125
0. 34	6.25
0.65	12.5
1.16	25
2.23	50
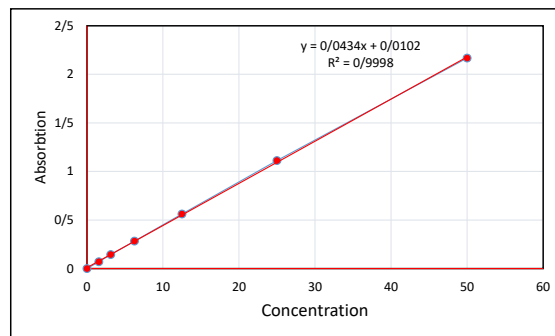
Figure 10. Calibration curve of loaded drug in acidic medium.

amount of drug measured in solution in the first 30 minutes was about 40%.

3.7. Drug release in acidic pH

Figures 10 and 11 show the amount of release (drug) in an acidic medium. As can be seen in this figure, the release rate of the drug in the zeolite sample is initially very high and decreases over time. In the sample containing zeolite, the amount of drug measured in solution in the first 30 minutes was about 12%. In long periods, the amount of drug measured in the medium due to the presence of zeolite was up to 17% more than the control sample.

The changes observed in the control sample can be attributed to the fact that a large part of the drug composition is initially destroyed due to their sensitivity to the acidic medium and the lack of zeolite preservatives. In the case of the zeolite sample, at the first moment, only the drugs on the surface are exposed to the acid. Due to the buffering properties of zeolite, the presence of this material increases the pH of the medium. Changes in the acidic degree of the medium in the zeolite sample have been investigated and the results are presented. Decreasing the acidity of the medium
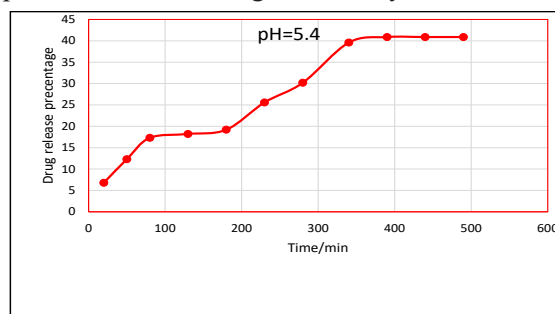
Figure 11. Diagram of drug release from nano carrier in acidic medium.

over time, has resulted in the stability of the folic acid released into the aqueous medium. Absorption amount of drug loaded on nano zeolite in different concentration in acidic medium mentioned in table 3.

High porosity composite zeolite has always been used as a carrier material to protect various organic compounds and has recently been proposed in pharmaceutical applications.

According to the diagrams 9, the percentage of gradual release of the drug from the nano carrier at 37 °C in simulated pH phosphate buffer solution (stomach=5.4) and (intestine=8.9) was observed in the first hour, 13% and 40% have been released, respectively. Then, by the end of the release time, the drug release gradually increases and then stops. In the simulation, the alkaline pH of the small intestine showed a sharp increase compared to the acidic conditions of the stomach. The slowest release was observed at pH 5.4 (stomach medium) and the fastest release was observed at pH 8.9 (small intestine medium).

4. Conclusion

Due to the interaction between the surface and inside of nano pores and the study compound, we see the gradual release of the compound from the surface of the nano carrier and also because the interaction is a hydrogen bond type, the release rate can be adjusted and controlled by changing the pH. On the other hand, by activating these nano carriers, the percentage of drug encapsulation can be increased. In general, it can be concluded that the nano carrier, due to its unique physical and chemical properties, acts as an effective nano carrier in the loading and gradual release of folic acid. Therefore, this nanostructure can be used as an intelligent nano carrier with the pH control release, which has the ability to protect the structure of various drugs to pass the drug through the acidic conditions of the stomach and transfer it to the intestine.

Conflict of Interest

There is no conflict of interest in this study.

References

1. Santos, H. A., Bimbo, L. M., Peltonen, L., Hirvonen, J., "Targeted Drug Delivery: Concepts and Design", Part VI, 1st edition, Springer International Publishing (CRS), Boston, USA, 571-613, (2015).

2. Kumar R, Lal S. Synthesis of Organic Nanoparticles and their Applications in Drug Delivery and Food Nanotechnology: A Review. *J Nanomater Mol Nanotechnol.* 2014;3:4. doi:10.4172/2324-8777.1000150

3. Wang R, Zhang Y, Lu D, Ge J, Liu Z, Zare RN. Functional protein-organic/inorganic hybrid nanomaterials. *Wiley Interdiscip Rev Nanomed Nanobiotechnol.* 2013 Jul-Aug;5(4):320-8. doi: 10.1002/wnan.1210. Epub 2013 Jan 29. PMID: 23362008.

4. Dizaj SM, Jafari S, Khosroushahi AY. A sight on the current nanoparticle-based gene delivery vectors. *Nanoscale Res Lett.* 2014 May 21;9(1):252. doi: 10.1186/1556-276X-9-252. PMID: 24936161; PMCID: PMC4046008.

5. Gregory AE, Titball R, Williamson D. Vaccine delivery using nanoparticles. *Front Cell Infect Microbiol.* 2013 Mar 25;3:13. doi: 10.3389/fcimb.2013.00013. PMID: 23532930; PMCID: PMC3607064.

6. Soppimath KS, Aminabhavi TM, Kulkarni AR, Rudzinski WE. Biodegradable polymeric nanoparticles as drug delivery devices. *J Control Release*. 2001 Jan 29;70(1-2):1-20. doi: 10.1016/s0168-3659(00)00339-4. PMID: 11166403.

7. Brigger I, Dubernet C, Couvreur P. Nanoparticles in cancer therapy and diagnosis. *Adv Drug Deliv Rev*. 2002 Sep 13;54(5):631-51. doi: 10.1016/s0169-409x(02)00044-3. PMID: 12204596.

8. Yuan F, Leunig M, Huang SK, Berk DA,

Papahadjopoulos D, Jain RK. Microvascular permeability and interstitial penetration of sterically stabilized (stealth) liposomes in a human tumor xenograft. *Cancer Res.* 1994 Jul 1;54(13):3352-6. PMID: 8012948.

9.	Storm G, Belliot SO, Daemen T, Lasic DD. Surface modification of nanoparticles to oppose uptake by the mononuclear phagocyte system. *Adv Drug Deliv Rev*. 1995;17:31-48.

10.	Chen H, Langer R. Oral particulate delivery: status and future trends. *Adv Drug Deliv Rev*. 1998 Dec 1;34(2-3):339-350. doi: 10.1016/s0169-409x(98)00047-7. PMID: 10837685.

11.	Desai MP, Labhasetwar V, Walter E, Levy RJ, Amidon GL. The mechanism of uptake of biodegradable microparticles in Caco-2 cells is size dependent. *Pharm Res.* 1997 Nov;14(11):1568-73. doi: 10.1023/a:1012126301290. PMID: 9434276.

12.	Win KY, Feng SS. Effects of particle size and surface coating on cellular uptake of polymeric nanoparticles for oral delivery of anticancer drugs. *Biomaterials*. 2005 May;26(15):2713-22. doi: 10.1016/j.biomaterials.2004.07.050. PMID: 15585275.

13.	Jin C, Bai L, Wu H, Song W, Guo G, Dou K. Cytotoxicity of paclitaxel incorporated in PLGA nanoparticles on hypoxic human tumor cells. *Pharm Res*. 2009 Jul;26(7):1776-84. doi: 10.1007/s11095-009-9889-z. Epub 2009 Apr 21. PMID: 19384463.

14.	Bhardwaj V, Hariharan S, Bala I, Lamprecht A, Kumar N, Panchagnula R, et al. Pharmaceutical aspects of polymeric nanoparticles for oral drug delivery. *J Biomed Nanotechnol.* 2005;1:235-58.

15.	Chai Y, Dai W, Wu G, Guan N, Li L. Confinement in a Zeolite and Zeolite Catalysis. *Acc Chem Res*. 2021 Jul 6;54(13):2894-2904. doi: 10.1021/acs.accounts.1c00274. Epub 2021 Jun 24. PMID: 34165959.

16.	Ming DW, Mumpton FA. Zeolites in Soils. In Minerals in Soil Environments (eds J.B. Dixon and S.B. Weed). 1989; Dixon J. B. & Weed S.B. (1992). Wisconsin, USA.) pp 873-911. https://doi.org/10.2136/sssabookser1.2ed.c18

17.	Tomlinson, AAG: (1998). Modern zeolites, structure and function in detergents and perto-chemicals. Trans techLtd UK. pp 1-16.

18.	Clifton, RA. (1985). Natural and synthetic zeolites. International Circular 9140. Washington, D.C.1. pp 24-118.

19.	Mumpton FA, Fishman PH. The application of natural zeolites in animal science and aquaculture. *J Anim Sci*. 1977;45:1188-1203.

20.	Ames LL. TThe Cation Sieve Properties of Clinoptilolite. *Amer Mineral.* 1960;45(5-6): 689-700.

21	Lam A, Rivera A, Rodrídguez-Fuentes G. Theoretical study of metronidazole adsorption on clinoptilolite. *Microporous Mesoporous Mater*. 2001;49(1-3): 157-162.

22.	Horcajada P, Márquez-Alvarez C, Rámila A, Pérez-Pariente J, Vallet-Regí M. Controlled release of Ibuprofen from dealuminated faujasites. *Solid State Sci.* 2006;8(12): 1459-1465.

23.	Wernert V, Schäf O, Ghobarkar H, Denoyel R. Adsorption properties of zeolites for artificial kidney applications. *Microporous Mesoporous Mater*. 2005;83(1-3): 101-113.

24.	Rodríguez-Fuentes G, Denis AR, Barrios Álvarez MA, Colarte AI. Antacid drug based on purified natural clinoptilolite. *Microporous Mesoporous Mater*. 2006;94(1-3): 200-207.

25.	Magdalena, T. Purification of natural zeolite-clinoptilolite for medical application-Extraction of lead. *J Serbian Chem Soc*. 2005;70. doi:10.2298/JSC0511335T.

26.	Institute of Medicine (US) Panel on Dietary Antioxidants and Related Compounds. Dietary Reference Intakes for Vitamin C, Vitamin E, Selenium, and Carotenoids. Washington (DC): National Academies Press (US); 2000. PMID: 25077263.

27.	Ersoy B, Çelik MS. Electrokinetic properties of clinoptilolite with mono- and multivalent electrolytes. *Microporous Mesoporous Mater*. 2002;55:305-312.

28. Azizian J, Mohammadi MK, Firuzi O, Mirza B, Miri R. Microwave-assisted solvent-free synthesis of Bis(dihydropyrimidinone) benzenes and evaluation of their cyto-toxic activity. *Chem Biol Drug Des.* 2010 Apr;75(4):375-80. doi: 10.1111/j.1747-0285.2009.00937.x. Epub 2010 Jan 19. PMID: 20102370.

29. Miri R, Razzaghi-asl N, Mohammadi MK. QM study and conformational analysis of an isatin Schiff base as a potential cytotoxic agent. *J Mol Model.* 2013 Feb;19(2):727-35. doi: 10.1007/s00894-012-1586-x. Epub 2012 Sep 29. PMID: 23053004.

30. Karimipour Z, Jalilzadeh Yengejeh R, Haghighatzadeh A, et al. UV-Induced Photo-degradation of 2,4,6-Trichlorophenol Using Ag–Fe2O3–CeO2 Photocatalysts. *J Inorg Organomet Polym.* 2021;31:1143-1152. https://doi.org/10.1007/s10904-020-01859-1

31. Zangeneh A, Sabzalipour S, Takdatsan A, Jalilzadeh Yengejeh R, Abullatif Khafaie M. Ammonia removal form municipal waste-water by air stripping process: An experimental study. *S Afr J Chem Eng.* 2021;36:134-41.

32. Liu J, Cui L, Losic D. Graphene and graphene oxide as new nanocarriers for drug delivery applications. *Acta Biomater.* 2013;9(12):9243-9257.

33. Pei X, Zhu Z, Gan Z, Chen J, Zhang X, Cheng X, et al. PEGylated nano-graphene oxide as a nanocarrier for delivering mixed anticancer drugs to improve anticancer activity. *Sci Rep.* 2020 Feb 17;10(1):2717. doi: 10.1038/s41598-020-59624-w. PMID: 32066812; PMCID: PMC7026168.

34. Sun X, Liu Z, Welsher K, Robinson JT, Goodwin A, Zaric S, Dai H. Nano-Graphene Oxide for Cellular Imaging and Drug Delivery. *Nano Res.* 2008;1(3):203-212. doi: 10.1007/s12274-008-8021-8. PMID: 20216934; PMCID: PMC2834318.

35. de Sousa M, Visani de Luna LD, Fonseca L, Giorgio S, Luiz Alves O. Folic-Acid-Functionalized Graphene Oxide Nanocarrier: Synthetic Approaches, Characterization, Drug Delivery Study, and Antitumor Screening. *ACS Applied Nano Material.* 2018;1(2):922-932.